Active Power Modulation Assisting Controller Scheme Implemented on a VSC-HVDC Link Establishing Effective Damping of Low Frequency Power Oscillations

Melios Hadjikypris [#1], Vladimir Terzija[#2]

[#] *Department of Electrical Energy and Power Systems, The University of Manchester, School of Electrical and Electronic Engineering, Ferranti Building, Sackville Street, Manchester, M13 9PL, United Kingdom*

[1] Melios.Hadjikypris@manchester.ac.uk

[2] Vladimir.Terzija@manchester.ac.uk

***Abstract*—Inter-area power oscillations damping is of fundamental importance in today's era of sophisticated and highly complex smart grids. The present paper demonstrates a practical solution obtaining satisfactory performance in damping power system oscillations utilizing the flexible VSC-HVDC transmission technology in an optimal combination with a power oscillation damping (POD) controller, utilizing active power modulation technique. Primary focus of the control scheme is to improve damping of lightly damped or even unstable modes of the interconnected AC/DC power system through modal analysis technique and a residue based approach. The proposed control scheme guarantees stability margins through eigenvalue analysis and non-linear time domain simulations, which are performed on a four-machine two-area system. The software platform under which the various simulation scenarios were implemented was DigSILENT PowerFactory.**

Keywords: **Low Frequency Power Oscillations, Inter-area oscillatory modes, Power Oscillation Damping, POD controller, VSC-HVDC, Eigenvalue analysis, Residues, DigSILENT PowerFactory.**

I. INTRODUCTION

In today's era of advanced technological intelligence, Cybernet and advanced automations, electrical power networks play a key role towards a smarter and greener sustainable future of the modern world [1]-[3].

A future smart grid must comply specific requirements associated with reliability, robustness and protection. A viable solution to this challenge is found in the recent advancements in high speed power electronics which soon enough gave rise to flexible AC transmission system (FACTS) devices [4]-[5]. A powerful tool that accomplish enhanced static and dynamic performance of the power system is the use of HVDC transmission technology, in fact Voltage Sourced Converter (VSC) based [6]-[7]. The fast power electronic switches of the Insulated Gated Bipolar Transistors (IGBTs), (constituting the core mechanism of VSCs along with pulse width modulation PWM technique), enables the self-commutated power converters to promptly and independently control the active and reactive power flows in the power system. This in turn boosts system's power transfer capability and stability performance during transient periods. The potentials provided by VSC-HVDC technology were very soon adopted by ABB and Siemens, under the code names HVDC Light® and HVDC PLUS [8], [9].

However, through the years of power systems evolution, a persistent challenge for system operators is associated with low frequency power oscillations developed in power systems [10]. The nature of these oscillations arises from lightly damped or even unstable local or inter-area oscillatory modes, under the case when the system experience small or large signal disturbances. Power oscillations appear as a result of inadequate damping torque of generators' rotors. The oscillating rotors in turn, develop the oscillations of other system's variables, such as active and reactive power flows, current flows, bus voltage magnitudes, phase angles, and electrical frequencies.

The low frequency electromechanical oscillations arise in a power system, are usually found in the range between 0.1-2Hz, depending on the number of contributing generators [11]. Local oscillations, which consist of oscillations of a single generator or a group of generators against the rest of the system, are usually found in the higher end of that range. Inter-area oscillations on the other hand, which occupy the lower end of frequencies (0.1-0.8 Hz) [12], are the oscillations associated between a group of generators in one area swinging against a group of generators in another area of the system.

In large interconnected power systems, poorly damped or even unstable inter-area oscillations usually occur between grids which are weakly connected. The weak connection refers to adjacent power grids connected over high impedance transmission lines, or transmission corridors subject to sudden and substantial change in power flow [13].

Over the years of innovation, substantial research has been undertaken in limiting the phenomena of inter-area oscillations, which span from instabilities, cascading events, or ultimate system blackouts (August/1996 western US/Canada interconnected system total blackout [13]).

The mitigation actions developed involve the applications of traditional power system stabilizers (PSSs) to counteract

oscillations from generators (local) point of view [14]. In addition, FACTS devices combined with power oscillation damping (POD) controllers (auxiliary control action) were also used for compensating oscillations from inter-area transmission point of view. The second approach has proven to achieve effective and powerful damping of oscillatory inter-area modes, as compared to generators' PSS point of view, which cannot really reach that performance satisfactorily. The application of POD supplementary control on FACTS devices gains significant popularity in the last few years. Examples can be found in Static VAr Compensators (SVCs), Thyristor Control Series Compensators (TCSCs), Unified Power Flow Controllers (UPFCs) and HVDC transmission technology [15]-[19].

Scope of this work is to combine the capabilities offered by VSC-HVDC technology (speed, flexibility, reliability) with the robustness and stabilizing actions obtained through POD control. This will result in overall system's damping improvement. This study is of critical importance because it looks into a field which lacks practical experience. This is a result of the dominant and well experienced current source converters (CSC) based HVDC installations worldwide [6], causing the VSC-HVDC technology to expand in a slow rate.

The analysis performed in this paper progresses in the following manner: Section II provides a brief overview of the dynamic modelling of VSC-HVDC transmission system. Section III details the test power system used to depict the various operational scenarios considered in this work, with the VSC-HVDC link in place. Following, in section (IV), the design considerations of the POD supplementary controller providing stabilizing actions to the VSC-HVDC link are presented. The simulation work undertaken in this paper, used to assess the dynamic performance of the control scheme, is summarised in section V. Finally, section VI draws all the conclusions and key points demonstrated in this paper.

II. VSC-HVDC MODELLING

The dynamic model of a VSC-HVDC transmission system is shown on figure 1. The diagram highlights the operational mechanism of the HVDC system, involving internal current control loop and external control loops.

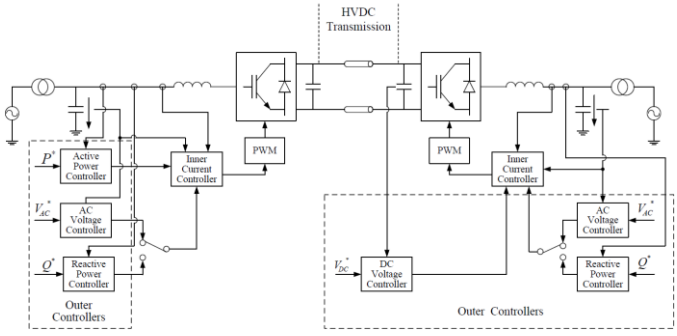

Fig. 1. VSC-HVDC transmission system dynamic model

According to figure 1, rectifier and inverter can be configured to control: active power flow (**P**) over the DC link, reactive power flow (**Q**) exchanged between the VSC converters and their corresponding AC grids, the DC link voltage ($\mathbf{V_{dc}}$), as well as the AC voltage ($\mathbf{V_{AC}}$) at the point of common connection (PCC) between a VSC converter and its adjacent AC grid. The fundamental control operation of the VSC-HVDC system is based on the vector control method [6]. This considers a rotating dq-reference frame for AC currents and voltages, at which its rotational speed matches the speed of AC current and voltage phasors ($\omega = 2\pi f$). This results both voltage and current variables to appear as constant vectors in the end. Based on this principle, simplified control mechanisms can be used to control dq current signals (i_d, i_q), and through these, the rest of system variables (**P**, **Q**, $\mathbf{V_{dc}}$, $\mathbf{V_{AC}}$). In this case, proportional integral (PI) controllers can be used to generate appropriate reference signals (i_d^{ref}, i_q^{ref}) for dq currents, through the use of selected system variables, as shown in figures 2-4.

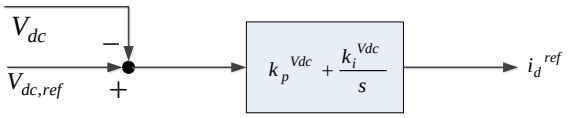

Fig. 2. DC voltage control loop

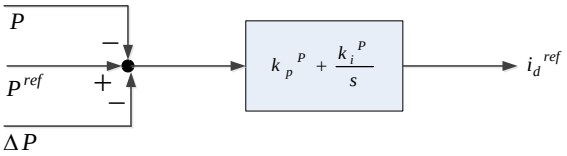

Fig. 3. Active power control loop

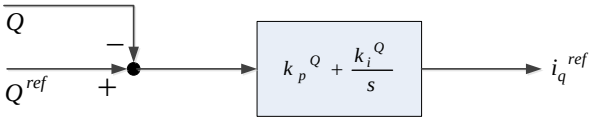

Fig. 4. Reactive power control loop

The designed VSC-HVDC system model incorporated in the test platform, is configured to control the DC link voltage ($\mathbf{V_{dc}}$) and reactive power flow (**Q**) through the rectifier. The inverter on the other hand, is set to control the active power flow **(P)** over the DC link, and corresponding reactive power (**Q**) exchanged by the converter. Further details regarding its topology and interconnection to the rest of the power system will follow on section III.

III. Power Network Test Platform

The operational test platform used to depict the various transient stability scenarios, under which the VSC-HVDC POD controller performance is assessed, is presented on figure 5. This emphasizes a single-line diagram of a well-studied four-machine two-area system, originally designed by Ontario Hydro [12], [25]. Objective of this system was to exhibit the different types of low frequency electromechanical oscillations develop in an interconnected power system. This is a benchmark system frequently used in inter-area oscillation studies. The system is symmetric through the interconnection of two identical areas over relatively weak tie-lines. As can be observed, the VSC-HVDC link is being incorporated in the two-area system. The full symmetry of the network, clarifies the effect the VSC-HVDC link with the POD controller have on the inter-area mode. In this case, the VSC-HVDC system provides a parallel transmission path (100 MW) across the long (220km) AC transmission corridor (between bus 3-5). Under steady state conditions, with normal network loading, roughly 400 MW active power is being transferred from area 1 to area 2 (left to right). Explicit system parameters (lines, transformers, shunt capacitors) and dynamic data (synchronous machines, AVRs, governors) can be found in [10], [12]. The generated power flows of the system can be seen on figure 5. It is worthwhile noting that no PSSs have been installed on generators, in order to highlight the stability provision accomplished by the auxiliary POD controller.

This system exhibits three electromechanical oscillatory modes. These are two local modes, one in which generator 1 swings against generator 2, and another in which generator 3 swings against generator 4. Additionally, there is one inter-area mode in which generators in area 1 swing against generators in area 2.

A. Two-Area System Technical Specifications

Generator 1 is assigned as a slack bus (SL) to the system, transmitting 750 MW of active power, whereas the rest generators are arrange into PV mode. Generators 2, 3, and 4 inject 700 MW, 719MW and 700MW of power respectively. All of them operate at a nominal AC voltage of 20kV (L-L) while rated at 900MVA. The four transformers are identically configured, stepping up the nominal voltage from 20kV to 230kV (L-L). Loads 1 and 2, (buses 3 and 5), consume 967 MW and 1767 MW of active power respectively. At the same time they both consume 100MVAr of reactive power. The loads are modelled as 50% dynamic (non-linear), and 50% static (constant impedance). Capacitors 1 and 2, both operated at a nominal voltage of 230 kV (L-L), are designed to inject 200MVAr and 350MVAr of reactive power to the network respectively, for maintaining voltage stability.

B. VSC-HVDC System Technical Specifications

The IGBT based power electronic converters consist the core operational mechanism of the VSC based system. Sinusoidal Pulse Width Modulation (PWM) technique is also used for transforming the control signals into electrical pulses feed in the transistors' gates.

Both VSC converters are operated at a nominal AC voltage of 230kV, and nominal DC voltage of 400kV, while having a rating of 300MVA apparent power.

As mentioned already, the rectifier is set to $\mathbf{V_{dc}}$-**Q** control mode. It maintains a stable DC voltage level on the HVDC corridor at 1.0 p.u., and at the same time retaining the reactive power flow to area 1 at 0 MVAr. The inverter of the system is arranged into **P-Q** control mode. This establishes a constant power flow of 100MW over the DC link, and zero reactive power to area 2. Details regarding the VSC-HVDC controllers' parameters can be found in the Appendix.

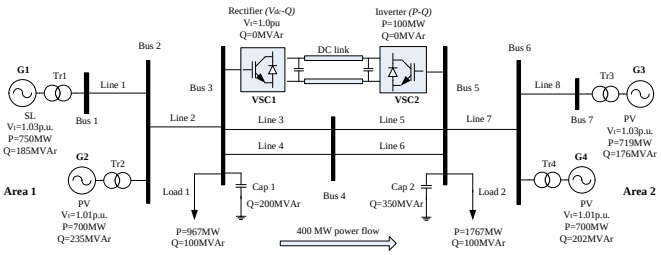

Fig. 5. Four-machine two-area test system incorporating VSC-HVDC transmission

IV. Supplementary POD Control: Design Methodology

In this section, the design procedure of the supplementary power oscillation damping (POD) controller assisting the power network compensating inter-area power oscillations will be presented. This utilizes the residue based tuning method for retrieving optimally tuned controller parameters [15], [16], [22].

A. The Residue Approach

Fundamental practice in addressing inter-area oscillations in a multi-machine system, is to first develop a complete linearized model of the actual system. This replaces the complexity of non-linear characteristics of the system with linear, and thus making our understanding of the system easier. In addition to this, tremendously reduces the design procedure of the auxiliary POD controller, since we adopt a linear design approach.

A linearized version of the 4-machine 2-area system incorporated with the VSC-HVDC link is given as follows [23]:

$$\begin{aligned} \Delta\dot{x} &= A\Delta x + B\Delta u \\ \Delta y &= C\Delta x + D\Delta u \end{aligned} \tag{1}$$

where A is the state variable matrix, B is the column-vector input matrix, and C the row-vector output matrix. Matrix D, that directly relates the input-output variables, is assumed to be zero. The complex eigenvalues reflecting the oscillatory behaviour of the above system always appear in complex conjugate form, such as $\lambda_i = \sigma_i \pm j\omega_i$. A pair of complex conjugate eigenvalues is also defined as an oscillatory mode. The real part (σ) represents the damping factor of the mode,

whereas the imaginary part (ω) the frequency of oscillation. The magnitude of the oscillation decays over time if σ is negative, while it increases if σ is positive. A practical measure for the assessment of oscillations is provided through the damping ratio (ζ), defined as:

$$\zeta = \frac{-\sigma}{\sqrt{\sigma^2 + \omega^2}} \times 100\% \tag{2}$$

For a power system, sufficient stability margins are established only when the damping ratios of the corresponding oscillatory modes are greater than 5% [10]. Modes characterized with lower damping ratios are defined as critical oscillatory modes. Poorly damped or unstable oscillations $(\zeta < 5\%)$ are a risk since they can lead to undesirable system conditions such as instabilities, cascading events, or ultimately catastrophic system blackouts.

The state matrix A of the system contains n distinct eigenvalues. The diagonal matrix of eigenvalues (Λ) along with the corresponding matrices of right (Φ) and left (Ψ) eigenvectors, satisfy the following set of matrix equations:

$$\begin{aligned} A\Phi &= \Phi\Lambda \\ \Psi A &= \Lambda\Psi \\ \Psi &= \Phi^{-1} \end{aligned} \tag{3}$$

A necessary condition in modifying a mode of oscillation through feedback control action is to choose an input signal capable of exciting the mode, and at the same time must be observable in the chosen output signal. The measures of these two properties are defined through the controllability (B') and observability (C') matrices, respectively given by:

$$\begin{aligned} B' &= \Phi^{-1}B \\ C' &= C\Phi \end{aligned} \tag{4}$$

The mode of interest is said to be uncontrollable if the row of the controllability matrix (B') corresponding to the specific mode is zero. Likewise, the mode is said to be unobservable if the corresponding column of matrix (C') is zero. In case where either of these two conditions hold true for the mode, then no feedback control action can really affect the mode.

Considering the case where the system described in equation (1) is single input single output (SISO). Then, its open loop transfer function is obtained by:

$$G(s) = \frac{\Delta y(s)}{\Delta u(s)} = C(sI - A)^{-1}B \tag{5}$$

This can be further expanded in the form of partial fractions, involving the input matrix B, the output matrix C, and the right and left eigenvectors as follows:

$$G(s) = \sum_{i=1}^{N} \frac{C\phi(:,i)\psi(i,:)B}{(s-\lambda_i)} = \sum_{i=1}^{N} \frac{R_i}{(s-\lambda_i)} \tag{6}$$

Each element in the numerator of every term is a scalar quantity named residue (R_i). The residue corresponding to each particular mode provides a measure of the mode's sensitivity to feedback control, between the input u and output y (concerning a SISO system). Finally, it is the product of mode's observability and controllability vectors.

Figure 6 below, illustrates the case where the system described by equation (5) is equipped with a negative feedback control action $H(s)$. The application of the feedback control causes the eigenvalues of the open loop transfer function $G(s)$ to shift. This change in system's eigenvalues is proved to be [15]:

$$\Delta\lambda_i = \Delta\sigma_i + j\Delta\omega_i = R_i H(\lambda_i) \tag{7}$$

As can be observed from the above expression, the geometrical distance of the shift of system's eigenvalue from its original position, is directly proportional to the residue's and controller's magnitudes $(|R_i|, |H_i|)$. An ideal damping to be achieved on the mode of interest, must shift the selected eigenvalue directly towards the left half of the complex plane, moving parallel to the real axis (preserving constant frequency (ω)).

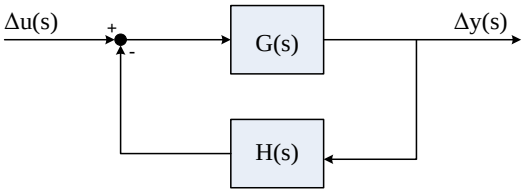

Fig. 6. Closed-loop system with POD feedback control

B. Residue Based VSC-HVDC POD Controller Design

Supplementary control action applied to the VSC-HVDC link for improving overall system's damping is called Power Oscillation Damping (POD) control. This can be seen on figure 6, where $G(s)$ represents the open-loop transfer function of the power system (including the VSC-HVDC transmission), whereas $H(s)$ reflects the POD VSC-HVDC controller. The auxiliary control action $H(s)$ was implemented based on the residue method analyzed above.

The scope of employing POD controller is to shift the real component $(\Delta\sigma_i)$ of the eigenvalue corresponding to the oscillatory (inter-area) mode of interest, further to the left-half of the complex plane. This results into improved damping. It can be achieved through a transfer function $H(s)$, which adopts the design proposed by [10], [15], [16], and its block diagram is demonstrated on figure 7. As can be observed, it

consists of a constant amplification gain (k_d), a lows-pass filter (T_m), a wash-out filter (T_w), and a series of phase compensation blocks ($T_{lead} - T_{lag}$), (usually one or two) [16].

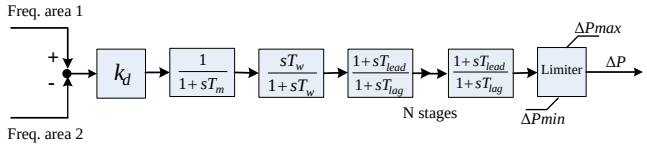

Fig. 7. Block diagram of a feedback power oscillation damping controller

The input of the supplementary damping controller is the frequency difference between area 1 and area 2, (see Fig. 5). One frequency is measured at bus 3 and the other one is measured at bus 5. The output of the controller (ΔP) is feed as an auxiliary signal to the inverter (VSC2) (See Fig. 3), and is used to modulate its active power reference. This will enable corresponding changes to be made in the active power flow over the DC link, in such a way as to damp inter-area oscillations.

In practise, the selection of the input signal is not unique. Other oscillatory signals could be used, such as power angles, active powers or currents across the AC inter-tie lines, voltage magnitudes or phase angles at the ends of the AC inter-tie lines, and rotor angles and generator speeds. The inter-area oscillation is associated with the differences between the rotor speed changes of different groups of generators. These changes can be clearly observed by monitoring system frequencies at different locations. Hence, the frequency difference between the two areas is a suitable choice for the input signal.

Considering figure 7, the transfer function obtained for the VSC-HVDC POD controller, $H(s)$, is given by:

$$H(s) = k_d \left(\frac{1}{1+sT_m} \right) \left(\frac{sT_w}{1+sT_w} \right) \left(\frac{1+sT_{lead}}{1+sT_{lag}} \right)^N \tag{8}$$

where k_d is a positive constant gain, T_m is the time constant of the low-pass filter, (typically 0.1s), and T_w is the washout time constant (usually 5-10s) [16]. Lastly, T_{lead} and T_{lag} are the lead and lag time constants of the *N*-phase compensation blocks.

As already stated, the geometrical distance of the shift ($\Delta\lambda_i$) of an eigenvalue is depended on both $|R_i|$ and $|H_i|$. The direction of this shift however, depends on the residue's phase angle, θ_R, and the phase shift across $H(s)$, $\varphi_{H(s)}$. Therefore, the ideal damping requirement mentioned earlier, must satisfy a summation of the two angles that will rotate the eigenvalue towards the left-half complex plane, moving parallel to the real axis, i.e., $\theta_R + \varphi_{H(s)} = 180°$.

The compensation angle $\varphi_{H(s)}$ is predominantly determined by the phase compensation blocks. The lead-lag parameter values, which will properly define the phase blocks, are obtained through the following set of equations:

$$\mathrm{N} = \begin{cases} 1 & \varphi_{\mathrm{H(s)}} \le 60^\circ \\ 2 & \varphi_{\mathrm{H(s)}} \le 140^\circ \end{cases} \tag{9}$$

$$\alpha = \frac{T_{lead}}{T_{lag}} = \frac{1-\sin\left(\frac{\varphi_{H(s)}}{N}\right)}{1+\sin\left(\frac{\varphi_{H(s)}}{N}\right)} \tag{10}$$

$$T_{lag} = \frac{1}{\omega\sqrt{\alpha}}, \quad T_{lead} = \alpha T_{lag} \tag{11}$$

where N is the number of compensation stages, and ω is the oscillation frequency (rad/s) of the mode to be modified.

C. Application to Two-Area Test System

Under steady-state conditions with standard network loading, our test system exhibits one critical inter-area oscillatory mode, with eigenvalue $\lambda_{\mathrm{int}} = -0.0944 + j3.3819$ and damping ratio of $\zeta = 2.79\% < 5\%$.

The POD controller illustrated above was applied into the VSC-HVDC link, to modulate the active power reference of the inverter (VSC2). However, in order first to calculate the residue's phase angle (θ_R) of the inter-area mode, the POD controller is only implemented with a constant gain (k_d), a low-pass filter $T_m = 0.1s$ and a wash-out filter $T_w = 10s$. No phase compensation blocks are involved at the moment. For different gain values, the inter-area mode must move in a straight line direction, as defined by the residue.

Modal analysis was performed under the cases were $k_d = 0$ and $k_d = 10$. The corresponding locations of the eigenvalues associated with the inter-area mode were recorded and the results are displayed on figure 8.

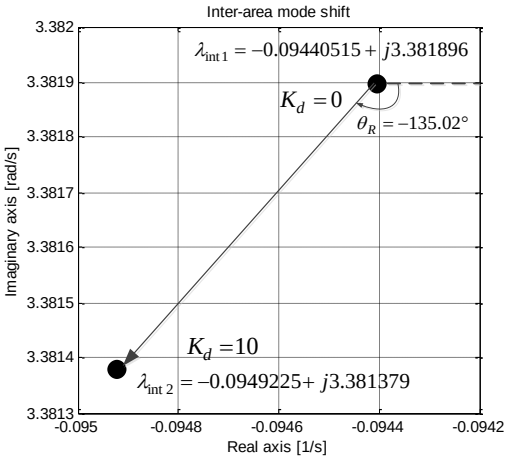

Fig. 8. Residue's phase angle estimation for POD controller design

As figure 8 suggests, the residue's phase angle was estimated to be $\theta_R = -135.0283°$. In this case, a positive feedback control is applied instead of negative (see Fig. 6). To design an ideal feedback controller (according to eq. (8)), the phase compensation blocks of the feedback controller, should introduce a phase shift of $\varphi_{H(s)} = +135.0283°$ at $0.54Hz = 3.381896 rads^{-1}$ (the frequency of the inter-area mode). Employing equations (9)-(11), and substituting $\omega = 3.381896 rads^{-1}$, the lead-lag parameter values that deliver such a phase shift are found to be: $T_{lead} = 0.0588s$ and $T_{lag} = 1.4878s$. Hence, the transfer function of the positive feedback POD controller is given by:

$$H(s) = k_d \left(\frac{1}{1+0.1s}\right)\left(\frac{10s}{1+10s}\right)\left(\frac{1+0.0588s}{1+1.4878s}\right)^2 \qquad (12)$$

A suitable choice of the gain k_d will be obtained through modal analysis that will follow, and the resulting controller's performance will be tested through time-domain non-linear simulations.

V. Simulation Studies

Having integrated the VSC-HVDC POD controller into the system, a modal analysis was performed under steady state conditions to identify the system's oscillatory modes. Analysis of the participations factors, categorize the modes into local, inter-area, exciter, governor and POD control. Figure 9, demonstrates the eigenvalues associated with all oscillatory modes, for different controller gains. In total, there are 9 oscillatory modes in the system. These consist of 4 exciter, 1 governor, 2 local, 1 inter-area, and 1 control modes. They are all well damped except the inter-area mode. On the complex plane provided, only the eigenvalues with positive imaginary part are presented, as complex eigenvalues always occur in conjugate pairs.

As can be observed, the inter-area oscillatory mode and POD control mode are the most sensitive to changes in feedback controller's gain, as compared to the rest of the modes which are relatively insensitive. As the controller gain increases, $(k_d = 100-1000)$, the poorly damped inter-area oscillatory mode moves directly to the left, while at the same time the POD control mode moves directly to the right. From the modal analysis, it is evident that once the controller gain becomes $k_d = 410$, maximum damping is achieved on the inter-area mode $(\lambda_{\text{int}.new} = -1.041529 + j3.879466)$ resulting into a damping ratio of $\zeta = 25.93\%$. However, for a higher range of gain values $(k_d = 600-1000)$, the inter-area mode is observed to start moving backwards to the right, causing the damping ratio to reduce.

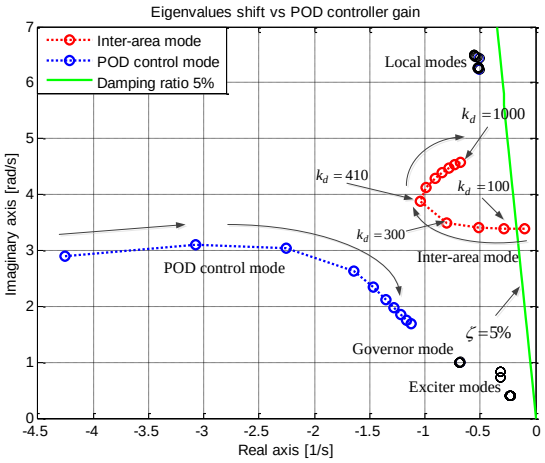

Fig. 9. Oscillatory modes versus the gain of the VSC-HVDC POD controller

In addition to the modal analysis performed on the test system, non-linear time domain simulations were followed, to test whether or not the designed POD controller properly damps inter-area oscillations. The simulation studies considered, involve small and large signal disturbances.

A. Small Signal Disturbance

In this case, an internal disturbance is developed in the system through a simultaneous change in the mechanical torques of two generators in the two separate areas. At time 0s, the mechanical torque of generator 2 was increased by 0.01p.u., whereas the corresponding torque of generator 4 was reduced by 0.01p.u. Figure 10 illustrates the responses of generator rotor speeds to the pair of disturbances, with and without the VSC-HVDC POD controller. Figure 11 on the other hand, shows the responses of the inter-area active power flow (line 3) to the small disturbance, for a variety of POD controller gains.

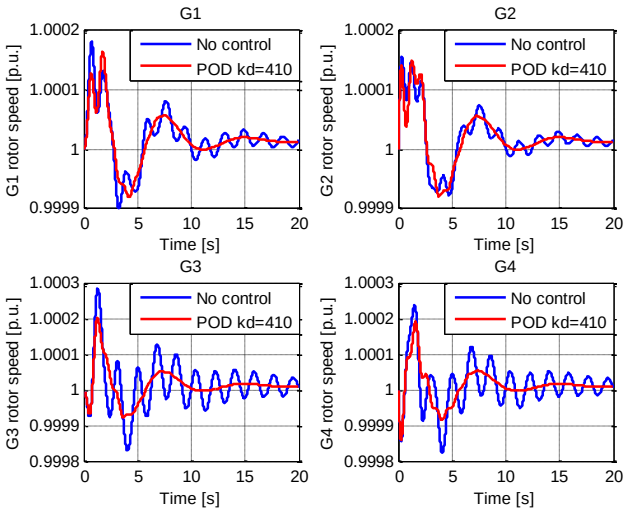

Fig. 10. Generator rotor speed responses to the small signal disturbance with and without supplementary VSC-HVDC POD controller

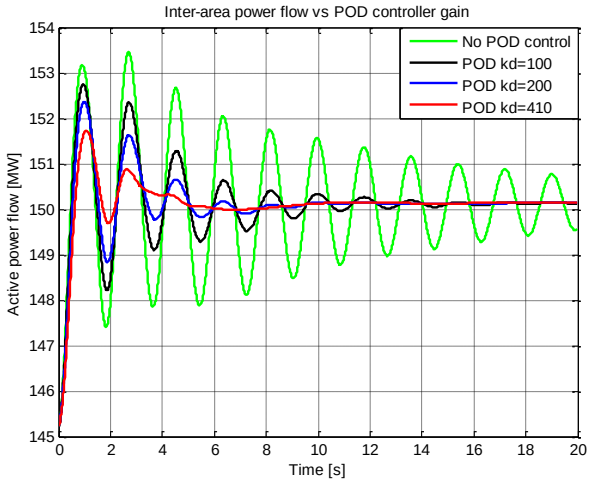

Fig. 11. Inter-area active power flow (line 3) responses to the small signal disturbance for a range of POD controller gains

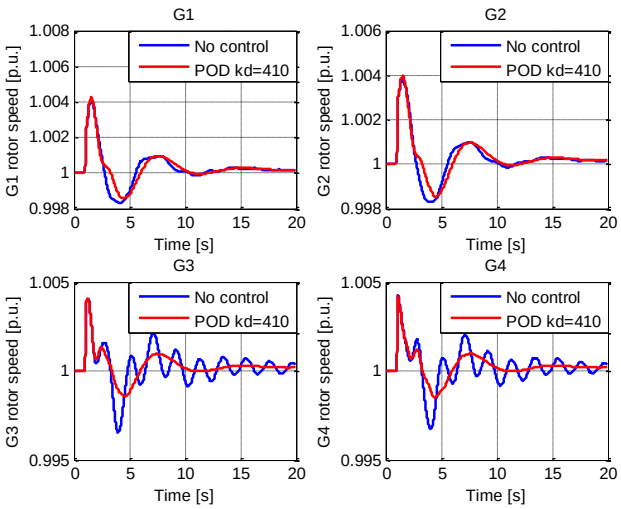

Fig. 12. Generator rotor speed responses to a three-phase fault with and without supplementary VSC-HVDC POD controller

Considering the obtained results represented by the above figures, it can be safely concluded that the POD controller manifests a powerful performance against small signal disturbances (develop in the power system) once optimally tuned. This was achieved through adequate damping established on the inter-area mode of oscillation. The optimal controller tuning (that gives the best performance), is highlighted on figure 11, where the damping accomplished on the inter-area mode was maximised at the corresponding gain value. It has been demonstrated that once appropriately tuned, the POD controller drastically assists the generators to promptly recover back to pre-disturbance operational speeds, in a much faster rate.

B. Large Signal Disturbance

The testing procedure of the POD controller is extended to involve a large disturbance event. This will be formed by a permanent three-phase short circuit fault initiated at the mid-point of line 6 (see Fig. 5). The faulted line is then disconnected from the system, 100ms following the fault. Figure 12 presents the responses of generator rotor speeds to the three-phase fault, with and without the VSC-HVDC POD controller.

It is evident from figure 12, that the VSC-HVDC POD controller has shown a remarkable performance in damping low frequency power oscillations, under the case when the system is subject to high disturbance. The controller's damping effect can be more vibrantly observed on generators closer to the disturbance, which in this case are generators 3 and 4. Figure 13, reflects the responses of the inter-area power flow (line 3) to the three-phase fault, under a variety of damping controller gains. As before, when the POD controller is increased (up to the maximum allowed value without sacrificing performance), the damping is equally increased. The damping effect is vigorous once optimal controller gain is selected.

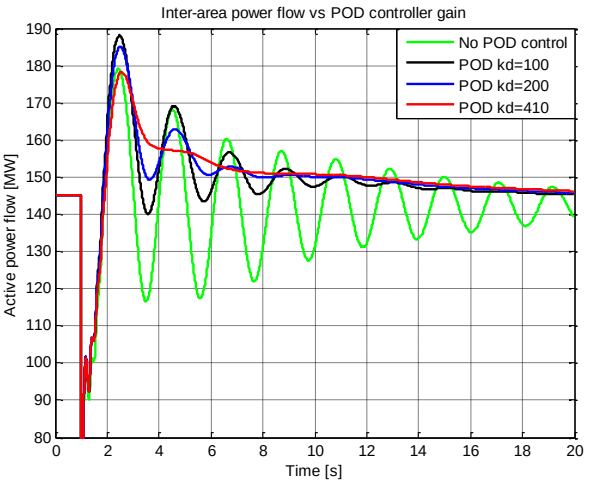

Fig. 13. Inter-area active power flow (line 3) responses to a three-phase fault for a range of POD controller gains

VI. CONCLUSION

The present study has demonstrated the design of a practical though powerful POD controller, for effectively damping low frequency inter-area power oscillations in an interconnected power system. The controller has utilized the traditional PSS structure that has been optimally integrated in a VSC-HVDC transmission system to modify its active power reference. This has result the direct control of active power flow over the DC link, and through this, the damping control provision on the inter-area mode. A careful selection of the controller's input signal is of crucial importance, since it must be able to excite the inter-area mode, and at the same time must be observable at the selected output signal. The selection of an input oscillatory signal comprising the oscillation phenomena developed in a diverse range in a system, results into the best possible robustness provision. The POD controller's design procedure was based on a 4-machine 2-area system, were modal analysis technique was employed for

guaranteed stability margins. Validation of controller's dynamic performance was established through non-linear time domain simulations. The simulation results have verified a remarkable controller's performance in damping low and high disturbance power oscillations, through robust and stable operation.

APPENDIX: VSC-HVDC CONTROLLER PARAMETERS

Rectifier: $k_p{}^{Vdc} = 1, k_i{}^{Vdc} = 0.1, k_p{}^{Q} = 0, k_i{}^{Q} = 0.1$

Inverter: $k_p{}^{P} = 0, k_i{}^{P} = 0.1, k_p{}^{Q} = 1, k_i{}^{Q} = 0.1$

ACKNOWLEDGMENT

The authors gratefully acknowledge the RCUK's Energy Programme for the financial support of this work through the Top & Tail Transformation programme grant, EP/I031707/1 (http://www.topandtail.org.uk/).

REFERENCES

[1] J. Kumagai, "The smartest, greenest grid," *Spectrum, IEEE* , vol.50, no.5, pp.42-47, May 2013.

[2] P. Chopade, S. Karagol, M. Bikdash, I. Kateeb, and N. Dogan, "Novel Smart Grid and SCADA system interdependency networks for future's clean, sustainable and green energy," *Emerging Technologies for a Smarter World (CEWIT), 2013 10th International Conference and Expo on* , vol., no., pp.1-6, 21-22 Oct. 2013.

[3] S. Keshav, and C. Rosenberg, "How internet concepts and technologies can help green and smarten the electrical grid", *In Proceedings of the first ACM SIGCOMM workshop on Green networking (Green Networking '10)*, New York, NY, USA, 2010, 35-40.

[4] V. K. Sood, *HVDC and Facts Controllers*, Springer, Inc., Publication 2004.

[5] R. Sadikovic, G. Andersson, P. Korba, "Power Flow Control with FACTS Devices", *World Automation Congress (WAC)*, Seville, 2004.

[6] J. Arrillaga, Y. H. Liu, N. R. Watson, *Flexible Power Transmission: The HVDC Options*, John Wiley & Sons, Inc. Publication 2007.

[7] N. Flourentzou, V.G. Agelidis, G.D. Demetriades, "VSC-Based HVDC Power Transmission Systems: An Overview," *Power Electronics, IEEE Transactions on*, vol.24, no.3, pp.592-602, March 2009.

[8] P. E. Bjorklund, K. Srivastava, W. Quaintance, "Hvdc Light® Modeling for Dynamic Performance Analysis," *Power Systems Conference and Exposition, 2006. PSCE '06. 2006 IEEE PES* , vol., no., pp.871-876, Oct. 29 2006-Nov. 1 2006.

[9] K. Friedrich, "Modern HVDC PLUS application of VSC in Modular Multilevel Converter topology", *Industrial Electronics (ISIE), 2010 IEEE International Symposium on* , vol., no., pp.3807-3810, 4-7 July 2010.

[10] G. Rogers, *Power System Oscillations*, Springer, Inc., Publication 1999.

[11] M. A. Pai and A. Stankovic, *Robust Control in Power System*, Springer Science+Bussiness Media, Inc. Publication 2005.

[12] P. Kundur, *Power System Stability and Control*, McGarw-Hill, Inc., Publication 1993.

[13] C.W. Taylor, "Improving grid behaviour", *IEEE Spectrum*, pp. 40-45, June 1999.

[14] P. Kundur, M. Klein, G.J. Rogers, M.S. Zywno, "Application of power system stabilizers for enhancement of overall system stability," *Power Systems, IEEE Transactions on* , vol.4, no.2, pp.614-626, May 1989

[15] M. E. Aboul-Ela, A. A. Sallam, J. D. McCalley, A. A. Fouad, "Damping controller design for power system oscillations using global signals," *Power Systems, IEEE Transactions on* , vol.11, no.2, pp.767-773, May 1996.

[16] R. Sadikovic, "Use of FACTS devices for power flow control and damping of oscillations in power systems," Ph.D thesis, Swiss Federal Institute of Technology Zurich, 2006.

[17] Y. F. Lin, Z. Xu, Y. Huang, "Power oscillation damping controller design for TCSC based on the test signal method," *Power Engineering Society General Meeting, 2005. IEEE* , vol., no., pp.1671-1675 Vol. 2, 12-16 June 2005.

[18] M. W. Mustafa, N. Magaji, "Design of power oscillation damping controller for SVC device," *Power and Energy Conference, 2008. PECon 2008. IEEE 2nd International* , vol., no., pp.1329-1332, 1-3 Dec. 2008.

[19] Y. Pipelzadeh, B. Chaudhuri, T. C. Green, "Wide-area power oscillation damping control through HVDC: "A case study on Australian equivalent system," *Power and Energy Society General Meeting, 2010 IEEE* , vol., no., pp.1-7, 25-29 July 2010.

[20] A. I. Stan and D. I. Stroe, "Control of VSC-based HVDC transmission system for offshore wind power plants", *Master Thesis*, Aalborg University, Denmark, September 2010.

[21] M. Klein, G. J. Rogers, P. Kundur, "A fundamental study of inter-area oscillations", *IEEE Trans. Power systems*, vol. 6, pp. 914-921, Aug. 1991.

[22] J. V. Milanovic and S. K. Yee, "Roadmap for tuning power system controllers", *3rd IASTED International Conference on Power and Energy Systems*, Marbella, Spain, September 2-4, 2003.

[23] K. Ogata, "*Modern Control Engineering*", Fifth Edition, Prentice Hall, Inc., Publication 2009.